Bench CJ, Friston KJ, Brown RG, Scott LC, Frackowiak RS, Dolan RJ. The anatomy of melancholia–focal abnormalities of cerebral blood flow in major depression. Psychological Medicine 1992;22:607–15.

Bench CJ, Frackowiak RS, Dolan RJ. Changes in regional cerebral blood flow on recovery from depression. Psychological Medicine 1995;25:79–85.

Brody AL, Saxena S, Silverman DH, Alborzian S, Fairbanks LA, Phelps ME, et al. Brain metabolic changes in major depressive disorder from pre- to post-treatment with paroxetine. Psychiatry Research 1999;91:127–39.

Buchsbaum MS, Wu J, Siegel BV, Hackett E, Trenary M, Abel L, et al. Effect of sertraline on regional metabolic rate in patients with affective disorder. Biological Psychiatry 1997;41:15–22.

Derogatis LR, Morrow GR, Fetting J, Penman D, Piasetsky S, Schmale AM, et al. The prevalence of psychiatric disorders among cancer patients. The Journal of the American Medical Association 1983;249:751–7.

Drevets WC, Videen TO, Price JL, Preskorn SH, Carmichael ST, Raichle ME. A functional anatomical study of unipolar depression. The Journal of Neuroscience 1992;12:3628–41.

Drevets WC, Price JL, Simpson Jr JR, Todd RD, Reich T, Vannier M, et al. Subgenual prefrontal cortex abnormalities in mood disorders. Nature 1997;386:824–7.

Drevets WC. Neuroimaging studies of mood disorders. Biological Psychiatry 2000;48:813–29.

Drevets WC, Bogers W, Raichle ME. Functional anatomical correlates of antidepressant drug treatment assessed using PET measures of regional glucose metabolism. European Neuropsychopharmacology 2002;12:527–44.

Dum RP, Strick PL. The origin of corticospinal projections from the premotor areas in the frontal lobe. The Journal of Neuroscience 1991;11:667–89.

Evans DL, McCartney CF, Nemeroff CB, Raft D, Quade D, Golden RN, et al. Depression in women treated for gynecological cancer. The American Journal of Psychiatry 1986;143:447–52.

Fawzy FI, Fawzy NW, Hyun CS, Elashoff R, Guthrie D, Fahey JL, et al. Malignant melanoma. Effect of an early structured psychiatric intervention, coping, and affective state on recurrence and survival 6 years later. Archives of General Psychiatry 1993;50:681–9.

Goodwin PJ, Leszcz M, Ennis M, Koopmans J, Vincent L, Guther H, et al. The effect of group psychosocial support on survival in metastatic breast cancer. The New England Journal of Medicine 2001;13(345):1719–26.

Hosaka T, Awazu H, Aoki T, Okuyama T, Yamawaki S. Screening of adjustment disorders and major depression in otolaryngology patients using the Hospital Anxiety and Depression Scale. International Journal of Psychiatry in Clinical Practice 1999;3:43–8.

Inagaki M, Matsuoka Y, Sugahara Y, Nakano T, Akechi T, Fujimori M, et al. Hippocampal volume and first major depressive episode after cancer diagnosis in breast cancer survivors. The American Journal of Psychiatry 2004;161:2263–70.

Katon W, Sullivan MD. Depression and chronic medical illness. The Journal of Clinical Psychiatry 1990;51: Suppl.3–11 discussion 12–4.

Kitamura T. Hospital Anxiety and Depression Scale. Seishinnkasinndanngaku 1993;4:371–2.

Krishnan KR, McDonald WM, Escalona PR, Doraiswamy PM, Na C, Husain MM, et al. Magnetic resonance imaging of the caudate nuclei in depression: preliminary observations. Archives of General Psychiatry 1992;49:553–7.

Levy SM, Herberman RB, Maluish AM, Schlien B, Lippman M. Prognostic risk assessment in primary breast cancer by behavioral and immunological parameters. Health Psychology 1985;4:99–113.

Levy S, Herberman R, Lippman M, d'Angelo T. Correlation of stress factors with sustained depression of natural killer cell activity and predicted prognosis in patients with breast cancer. Journal of Clinical Oncology 1987;5:348–53.

Maddock RJ. The retrosplenial cortex and emotion: new insights from functional neuroimaging of the human brain. Trends in Neurosciences 1999;22:310–6.

Matsui K, Fukuoka M, Masuda N, Kusunoki Y, Negoro S, Takada M, et al. High-dose Tegafur (FT) for primary lung cancer: a phase I trial. Gan To Kagaku Ryoho 1991;18(4):593–9.

McDaniel JS, Musselman DL, Porter MR, Reed DA, Nemeroff CB. Depression in patients with cancer. Diagnosis, biology, and treatment. Archives of General Psychiatry 1995;52:89–99.

Massie MJ, Holland JC. Depression and the cancer patient. The Journal of Clinical Psychiatry 1990;51:12–7.

Mayberg HS, Liotti M, Brannan SK, McGinnis S, Mahurin RK, Jerabek PA, et al. Reciprocal limbic-cortical function and negative mood: converging PET findings in depression and normal sadness. The American Journal of Psychiatry 1999;156:675–82.

Meltzer CC, Kinahan PE, Greer PJ, Nichols TE, Comtat C, Cantwell MN, et al. Comparative evaluation of MR-based partial-volume correction schemes for PET. Journal of Nuclear medicine 1999;40:2053–65.

Nakano T, Wenner M, Inagaki M, Kugaya A, Akechi T, Matsuoka Y, et al. Relationship between distressing cancer-related recollections and hippocampal volume in cancer survivors. The American Journal of Psychiatry 2002;159:2087–93.

Ongur D, Drevets WC, Price JL. Glial reduction in the subgenual prefrontal cortex in mood disorders. Proceedings of the National Academy of Sciences of the United States of America 1998;95:13290–5.

Petty F, Noyes Jr R. Depression secondary to cancer. Biological Psychiatry 1981;16:1203–20.

Phan KL, Wager T, Taylor SF, Liberzon I. Functional neuroanatomy of emotion: a meta-analysis of emotion activation studies in PET and fMRI. NeuroImage 2002;16:331–48.

Price JL, Carmichael ST, Drevets WC. Networks related to the orbital and medial prefrontal cortex: A substrate for emotional behavior?. Progress in Brain Research 1996;107:523–36.

Razavi D, Delvaux N, Farvacques C, Robaye E. Screening for adjustment disorders and major depressive disorders in cancer in-patients. The British Journal of Psychiatry 1990;156:79–83.

Roland PE, Eriksson L, Widen L, Stone-Elander S. Changes in regional cerebral oxidative metabolism induced by tactile learning and recognition in man. The European Journal of Neuroscience 1989;1:3–18.

Roland PE, Gulyas B, Seitz RJ, Bohm C, Stone-Elander S. Functional anatomy of storage, recall, and recognition of a visual pattern in man. Neuroreport 1990;1:53–6.

Sinha R, Lacadie C, Skudlarski P, Wexler BE. Neural circuits underlying emotional distress in humans. Annals of New York Academy of Sciences 2004;1032:254–7.

Smith KA, Morris JS, Friston KJ, Cowen PJ, Dolan RJ. Brain mechanisms associated with depressive relapse and associated cognitive impairment following tryptophan depletion. The British Journal of Psychiatry 1999;174:525–9.

Tashiro M, Juengling FD, Reinhardt MJ, Mix M, Kumano H, Kubota K, et al. Depressive state and regional cerebral activity in cancer patients – a preliminary study. Medical Science Monitor 2001;7:687–95.

Uchitomi Y, Fukase M, Sugihara J. A liason program influences psychiatric consultation rates in cancer patients at a Japanese general hospital. In: Seventh Annual Meeting of the European Society of Psychosocial Oncology, 1993; Abstract p. 99.

Wise SP. The primate premotor cortex: past, present, and preparatory. Annual Review of Neuroscience 1985;8:1–19.

Yoshikawa E, Matsuoka Y, Yamasue H, Inagaki M, Nakano T, Akechi T, et al. Prefrontal cortex and amygdala volume in first minor or major depressive episode after cancer diagnosis. Biological Psychiatry 2006;59(8):707–12.

Zigmond AS, Snaith RP. The hospital anxiety and depression scale. Acta Psychiatrica Scandinavica 1983;67:361–70.

Available online at www.sciencedirect.com
ScienceDirect
Neuroscience Letters 414 (2007) 99–104
Neuroscience Letters
www.elsevier.com/locate/neulet

Deactivation and activation of left frontal lobe during and after low-frequency repetitive transcranial magnetic stimulation over right prefrontal cortex: A near-infrared spectroscopy study

Naoki Hanaoka, Yoshiyuki Aoyama, Masaki Kameyama, Masato Fukuda*, Masahiko Mikuni

Department of Psychiatry and Human Behavior, Gunma University Graduate School of Medicine, 3-39-22 Showa-machi, Maebashi, Gunma 371-8511, Japan

Received 7 June 2006; received in revised form 11 September 2006; accepted 1 October 2006

Abstract

The effects of low-frequency repetitive transcranial magnetic stimulation (rTMS) over the right frontal lobe on the function of the left frontal lobe were examined by near-infrared spectroscopy (NIRS) in eleven healthy subjects. rTMS applied 5 cm anterior to the motor cortex at 1 Hz and approximately 50% of the motor threshold intensity (MT) for 60 s resulted in a significantly larger decrease in the concentration of oxygenated hemoglobin ([oxy-Hb]) during the stimulation period followed by a significantly larger increase in [oxy-Hb] and a smaller decrease in the concentration of deoxygenated hemoglobin ([deoxy-Hb]) during the poststimulation baseline period than sham stimulation. These findings are interpreted as demonstrating the deactivation and activation of the left frontal cortex during and after rTMS of the right frontal cortex, respectively. If replicated in depressed patients, NIRS can be employed for monitoring rTMS effects as brain [Hb] changes in vivo, and may be helpful for determining therapeutic parameters of rTMS for individual patients.

Keywords: rTMS; Near-infrared spectroscopy; Hemoglobin concentration; Depression; Magnetic stimulation; Therapy

Repetitive transcranial magnetic stimulation (rTMS) has been increasingly employed for the treatment of depression since it was first reported in 1996 [23], and its effectiveness has been demonstrated in several randomized trials [4,7,10,12,15]. Most of the studies on depression treatment used high-frequency rTMS delivered over the left prefrontal area [3] because depression is hypothesized to arise from dysfunction of the left prefrontal cortex [6] and high-frequency rTMS exceeding 1 Hz is considered to have a facilitatory effect on the brain stimulated [24].

However, high-frequency rTMS, in general, might be accompanied by a risk of inducing convulsions, as the most serious complications of rTMS [28], although this occurs very rarely when rTMS is conducted according to the safety guidelines for TMS experiments suggested by Wassermann [28]. Such a risk has led to an interest in a possible alternative rTMS method for depression treatment: low-frequency rTMS over the right prefrontal cortex. In fact, two recent reports demonstrated comparable antidepressant effects of low-frequency rTMS over the right prefrontal cortex and high-frequency rTMS over the left prefrontal cortex in depressed patients: 1 Hz rTMS over the right prefrontal cortex versus 10 Hz rTMS over the left prefrontal cortex [4] and 1 Hz rTMS over the right prefrontal cortex versus 20 Hz rTMS over the left prefrontal cortex [8].

Mechanisms underlying the antidepressant effects of rTMS have been examined using positron emission tomography (PET) and single-photon emission computerized tomography (SPECT), and the results generally demonstrated opposite directional changes between high- and low-frequency stimulations. rTMS over the left prefrontal cortex in depressed patients resulted in regional cerebral blood flow (rCBF) increases in the left prefrontal cortex and related brain structures when delivered at 20 Hz and in rCBF decreases in the right prefrontal cortex and left subcortical brain structures at 1 Hz in a PET study [26]. Sim-

* Corresponding author. Tel.: +81 27 220 8185; fax: +81 27 220 8187.
E-mail address: fkdpsy@med.gunma-u.ac.jp (M. Fukuda).

0304-3940/$ – see front matter © 2006 Elsevier Ireland Ltd. All rights reserved.
doi:10.1016/j.neulet.2006.10.002

ilarly, high- (15 Hz) and low-frequency (1 Hz) rTMS over the left prefrontal cortex in depressed patients resulted in an overall increase and a slight decrease in rCBF in the left dorsolateral prefrontal cortex and related brain structures, respectively, in a SPECT study [16].

Mechanisms underlying the antidepressant effects of rTMS have also been examined using near-infrared spectroscopy (NIRS), a recently developed technology that enables the assessment of cerebral blood volume (CBV) changes by monitoring the concentrations of oxygenated ([oxy-Hb]) and deoxygenated hemoglobin ([deoxy-Hb]) with high time resolution [11]. NIRS has two main advantages over PET, SPECT, and functional magnetic resonance imaging (fMRI) in investigating brain responses to TMS: its natural measurement setting with subjects in the sitting position and without requiring a gantry, and simultaneous measurement during rTMS.

Five studies that employed NIRS with TMS have been published. Single-pulse stimulation over the left motor cortex (M1) of healthy subjects was reported to cause [oxy-Hb] increases at 90 and 110% of active motor threshold intensity (AMT) [19] and [deoxy-Hb] decreases without [oxy-Hb] changes at 140% AMT [17]. rTMS over the right frontal cortex of healthy subjects was reported to increase [oxy-Hb] in the stimulated area immediately after the stimulation [22] and decrease [oxy-Hb] in the contralateral M1 during the stimulation in a preliminary study [9]. In depressed patients, smaller [Hb] changes attributable to a mental task were associated with subsequent better clinical responses to 10 Hz active rTMS [2].

NIRS data obtained simultaneously with rTMS may help in establishing the proper location and optimal intensity of rTMS in depression treatment. As far as we surveyed, however, there has been no NIRS study that examined the effect of low-frequency rTMS over the right frontal lobe on the left frontal lobe function changes induced by rTMS. Hence, in the present preliminary study, we investigated left frontal lobe function by NIRS during low-frequency rTMS over the right frontal lobe in healthy subjects.

Eleven healthy volunteers (10 males, 1 female) participated in the study after giving their written informed consent (Table 1). None of them had a personal or family history of convulsions or had pacemakers or metal hardware implanted in their skull. All the subjects were determined as right-handed on the basis of the Edinburgh Handedness Inventory [21]. The present study had been approved by the Institutional Review Board of the Gunma University Graduate School of Medicine, and all the experimental procedures strictly followed the safety guidelines for TMS experiments suggested both by Wassermann [28] and by the Japanese Society of Clinical Neurophysiology [1].

Table 1
Characteristics of subjects

No.	Sex	Age	Handedness	MT (%)
1	M	38	R (26)	52
2	M	35	R (36)	70
3	M	45	R (35)	77
4	M	29	R (36)	67
5	M	43	R (36)	66
6	M	29	R (27)	43
7	M	29	R (36)	53
8	M	31	R (36)	52
9	M	26	R (36)	77
10	M	27	R (36)	60
11	F	32	R (36)	72

The right M1 position was identified by single-pulse TMS, and the sites of frontal rTMS were determined as points 5 cm anterior to M1s as generally employed [6].

Under the active condition, rTMS was applied in three sessions without intervals using Magstim Rapid and a figure-of-8 coil (Magstim Company, UK). Each session consisted of a prestimulation baseline period of 20 s, an rTMS period of 60 s, and a poststimulation baseline period of 120 s. Stimulation frequency and intensity were set at 1 Hz and 100% MT, respectively. Stimulation intensities over the scalp, however, were confirmed to be reduced approximately 50% using the eXimia NBS system (Nexstim Ltd., Finland) because the TMS coil was set 1.5 cm apart from the scalp to avoid artifacts attributable to its contact with the NIRS probes. Therefore, the subjects neither had spasms nor felt pain under the active condition. We had confirmed the efficacy of 50% MT stimulation in our preliminary study: TMS at 50% MT, but not at 30% MT, causes the NIRS signal changes. Under the sham condition, a figure-of-8 coil positioned 50 cm behind the subjects was employed. Only click sounds, but no surface stimulation, were delivered. The subjects were required to copy a landscape picture or a cartoon on a PC screen during the three sessions according to the method of Watanabe et al. [29] to reduce sleepiness.

Brain activation during TMS was monitored by measuring [Hb] changes over the left hemisphere using a multichannel NIRS apparatus (ETG-100, Hitachi Medical, Japan) with a time resolution of 0.1 s. And its channel 1 corresponding to a symmetrically opposite TMS position (Fig. 1).

[Oxy-Hb] and [deoxy-Hb] data were averaged across three sessions within each subject for each channel after excluding

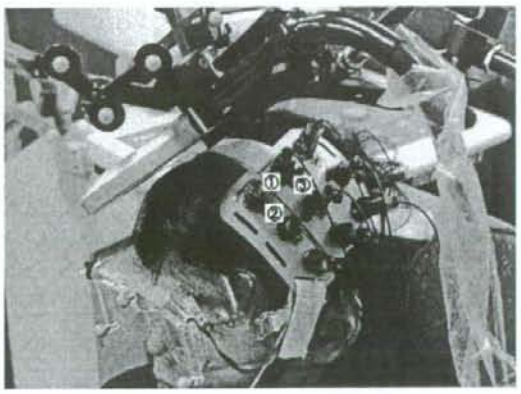

Fig. 1. Experimental setting. The rTMS coil was positioned over the right prefrontal cortex, and the NIRS probe was set over the left frontal lobe. NIRS measured hemoglobin concentration in three midpoints between emission and detector probes (channels 1, 2, and 3).

data with motion artifacts. The intraindividually averaged [Hb] data of all the subjects were grand-averaged, and then compared between the active and the sham stimulation conditions using the blocked and sequential paired *t*-test: the blocked *t*-test for the mean data across 60 s during the stimulation (block A) and the first half (block B) and the second half (block C) of the poststimulation period, and the sequential *t*-test for the data of every measurement point. Differences between the

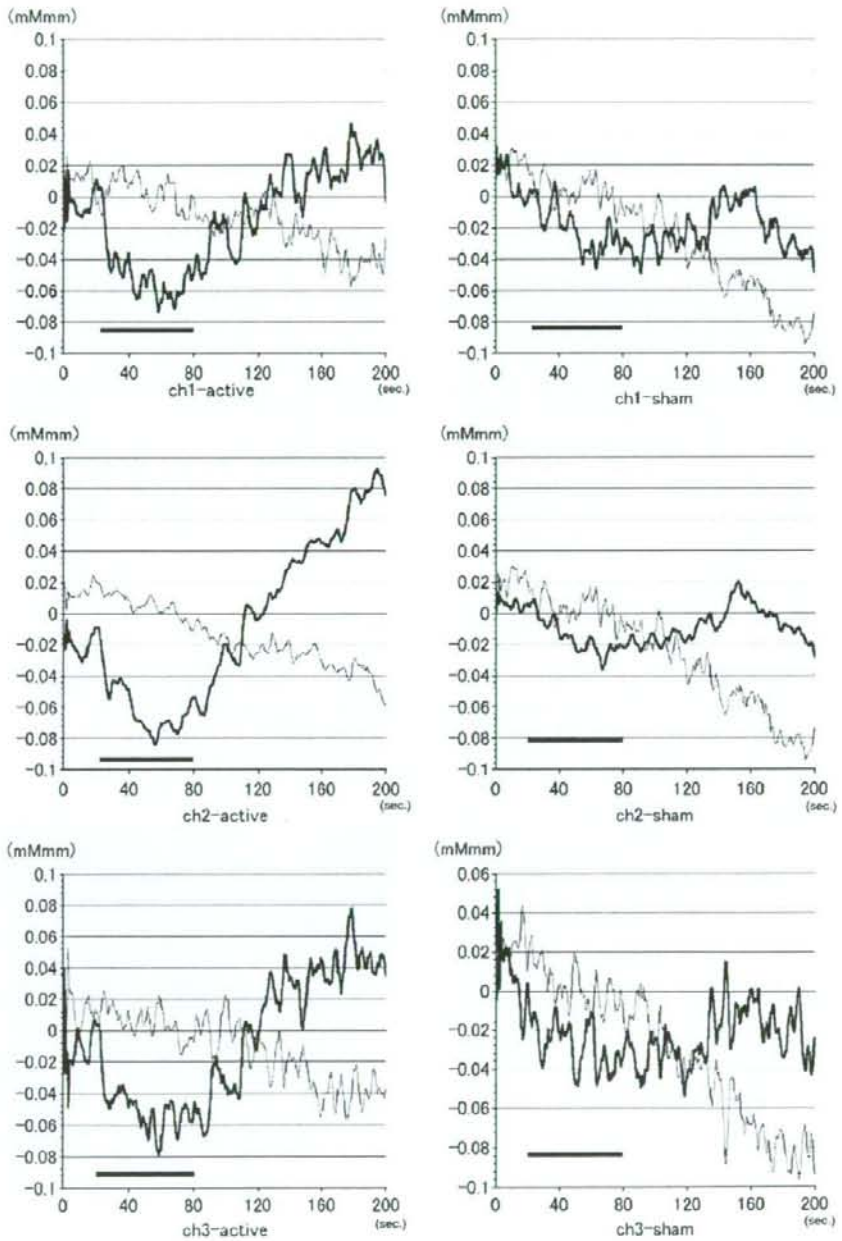

Fig. 2. Grand average waveforms of hemoglobin concentration changes. Grand average waveforms of [oxy-Hb] (thick line) and [deoxy-Hb] changes (thin line) before (0–20 s), during (20–80 s, gray bar), and after rTMS (80–200 s) in the active (left) and the sham conditions (right) from channels 1 (top), 2 (middle), and 3 (bottom).

two conditions were interpreted as statistically significant when they reached 1.7% of the significance in the blocked t-test and when they reached the 5% significance level across 50 consecutive points (5 s) during the stimulation and poststimulation periods in the sequential t-test for the correction of multiple comparisons.

All the subjects underwent the experiment without severe side effects.

The grand average [Hb] data of all the subjects are presented for three NIRS channels (Fig. 2) Under the active condition (Fig. 2, left), [oxy-Hb] decreased gradually during the stimulation period, then increased around the end of the stimulation period, continued to increase beyond the baseline, and peaked approximately 100–120 s after the end of stimulation. Under the sham condition (Fig. 2, right), similar but much smaller [oxy-Hb] changes were observed. As for [deoxy-Hb], constant decreases in [deoxy-Hb] were observed both under the active and sham conditions.

In the blocked t-test, [oxy-Hb] significantly decreased during the stimulation in channels 1 and 2 and tended to increase during the second half of the poststimulation in channels 2 and 3 (Fig. 3 upper). [Deoxy-Hb] changes were not statistically significant (Fig. 3 lower). In the sequential t-test, [oxy-Hb] decreases were significantly larger during the stimulation period in channel 1 (time, 33.9–39.2), channel 2 (times, 25.0–34.0 and 34.9–87.8), and channel 3 (time, 56.6–61.7), and [oxy-Hb] increases were significantly larger at the end of the poststimulation baseline period in channel 1 (time, 177.0–187.1 and 192.3–198.9), channel 2 (time, 175.0–200.0), and channel 3 (times, 152.0–159.1, 174.8–181.2 and 193.6–199.7) under the active than under the sham condition (Fig. 4). A similar paired t-test of [deoxy-Hb] demonstrated significantly smaller [deoxy-Hb] decreases during the poststimulation period in channel 1 (time, 119.9–125.3,) and channel 3 (times, 117.2–123.4 and 162.0–167.3) under the active than the sham condition (Fig. 5).

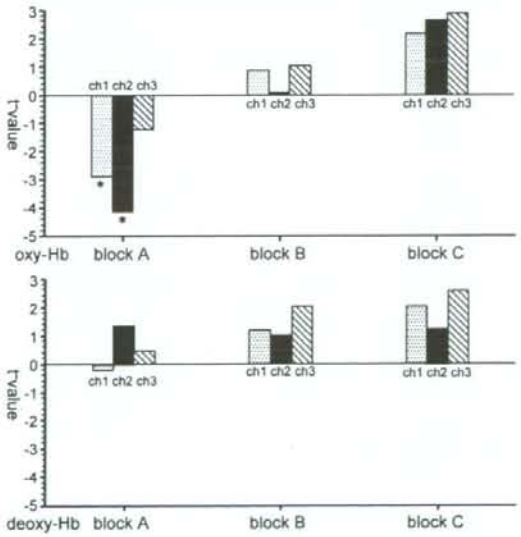

Fig. 3. Results of blocked t-test comparing [oxy-Hb] (upper) and [deoxy-Hb] (lower) between active and sham conditions. t-Value for the mean data across 60 s during the stimulation (block A) and the first half (block B) and the second half (block C) of the poststimulation period, Positive and negative values correspond to greater and smaller [Hb], respectively, in the active condition.

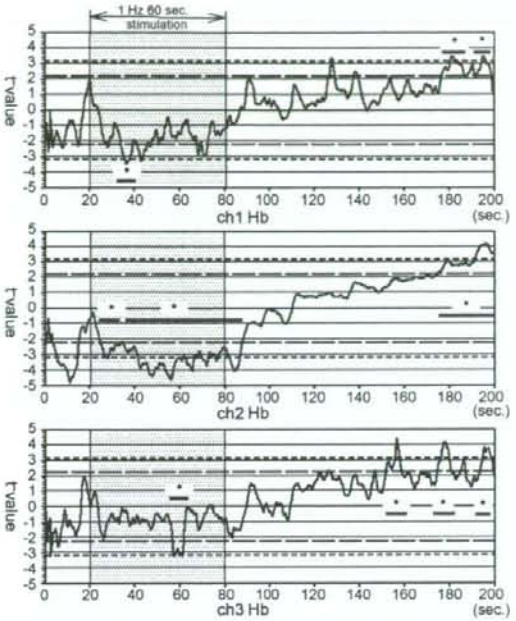

Fig. 4. Results of sequential paired t-test comparing [oxy-Hb] between active and sham conditions. t-Values are plotted along the time course of rTMS for channels 1 (top), 2 (middle), and 3 (bottom). Positive and negative values correspond to greater and smaller [oxy-Hb], respectively, in the active condition. Unadjusted significance levels of 5 and 1% are indicated by long and short broken lines, respectively.

In the present study, we investigated the left frontal lobe function changes during 1 Hz rTMS over the right frontal cortex in the healthy subjects using NIRS, and demonstrated significant larger [oxy-Hb] and smaller [deoxy-Hb] changes than under the sham condition: larger [oxy-Hb] decreases during the stimulation period and larger [oxy-Hb] increases and smaller [deoxy-Hb] decreases during the poststimulation baseline period. This is the first NIRS study carried out to examine brain activation in the hemisphere contralateral to that stimulated. Regrettably, direct NIRS measurement over the stimulated brain regions was not possible because of technical problems in TMS and NIRS probe positioning.

The effects of frontal TMS on the contralateral frontal lobe function have been investigated in sixteen studies, as far as we surveyed, using other technologies such as PET, SPECT, fMRI, and Doppler ultrasonography. Thirteen out of sixteen studies employed left frontal stimulation, two right frontal, and one both right and left stimulations. Left frontal stimulation resulted in inconsistent findings: for example, rCBF in the stimulated and

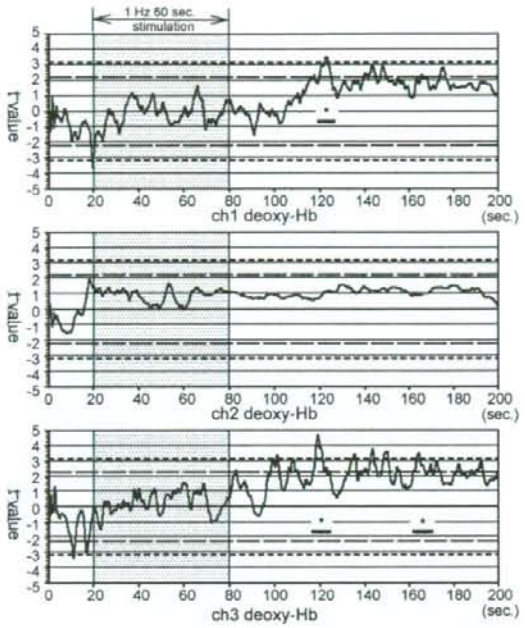

Fig. 5. Results of sequential paired *t*-test comparing [deoxy-Hb] between active and sham conditions illustrated as in Fig. 4.

contralateral prefrontal cortex was negatively correlates with rTMS intensity in a PET study (1 Hz; 80–120% MT) [27]; bilateral prefrontal activation was demonstrated by TMS over the left prefrontal cortex at 1 Hz-100% MT in two [14,18] and at 1 Hz-120% MT in one fMRI study [18]; CBF does not increase ipsilateral and decreases in the contralateral prefrontal cortex in a SPECT study [5]. Moreover, a PET study comparing high- and low-frequency stimulations over the left and right prefrontal cortices showed larger rCBF increases in the right PFC by 1 than 10 Hz left PFC stimulation, and rCBF increases in the left PFC by 1 Hz right PFC stimulation without any effect on the stimulated site [13].

These inconsistent results can be explained by differences in several factors among the studies.

Two right frontal stimulation studies demonstrated the same left frontal activation: Middle cerebral arterial blood flow velocity decreases and tends to increase in the ipsilateral and the contralateral hemispheres, respectively, 10 min after TMS over the right dorsolateral prefrontal cortex (0.9 Hz, 90% MT, 10 min) [25]. Cerebral blood flow increases in the ipsilateral and the contralateral hemispheres during and after TMS over the right dorsolateral prefrontal cortex (1 Hz, 100% MT, 100 stimuli) in a PET study [20].

The delayed activation of the contralateral hemisphere by prefrontal TMS in the above two studies is in agreement with the results of the present study, and is assumed to be important for considering the therapeutic effects of prefrontal rTMS in depression in two points. First, the finding that low-frequency rTMS over the right frontal cortex activated the left frontal cortex can explain the antidepressant effect of such type of rTMS because the left frontal lobe function is hypothesized to be impaired in depression [6]. Second, the delayed timing of the activation of the left frontal lobe can explain the time course of the antidepressant effect of frontal rTMS in depression. Depressed patients experience an improvement of depressive symptoms not during the stimulation but after TMS sessions. Such time course data can be obtained by virtue of the high time resolution of NIRS. Such delayed timing of activation could underlie the accumulated prefrontal activation in minute order by repeated TMS sessions in an fMRI study [14].

If the findings in the present study are replicated in depressed patients, NIRS can be employed for monitoring rTMS effects as brain [Hb] changes in vivo, and may be helpful for determining therapeutic parameters of rTMS for individual patients. Further studies are needed.

References

[1] Committee on the guidelines for transcranial magnetic stimulation in the Japanese Society of Clinical Neurophysiology, Recommendation on the safety of transcranial magnetic stimulation, Jpn J Clin Neurophsiol 31(2003) 69.

[2] G.W. Eschweiler, C. Wegerer, W. Schlotter, C. Spandl, A. Stevens, M. Bartels, G. Buchkremer, Left prefrontal activation predicts therapeutic effects of repetitive transcranial magnetic stimulation (rTMS) in major depression, Psychiatry Res. 99 (2000) 161–172.

[3] G.S. Figiel, C. Epstein, W.M. McDonald, J. Amazon-Leece, L. Figiel, A. Saldivia, S. Glover, The use of rapid-rate transcranial magnetic stimulation (rTMS) in refractory depressed patients, J. Neuropsychiatry Clin. Neurosci. 10 (1998) 20–25.

[4] P.B. Fitzgerald, T.L. Brown, N.A. Marston, Z.J. Daskalakis, A. De Castella, J. Kulkarni, Transcranial magnetic stimulation in the treatment of depression: a double-blind, placebo-controlled trial, Arch. Gen. Psychiatry 60 (2003) 1002–1008.

[5] M.S. George, L.E. Stallings, A.M. Speer, Z. Nahas, K.M. Spicer, D.J. Vincent, D.E. Bohning, K.T. Cheng, M. Molloy, C.C. Teneback, S.C. Risch, Prefrontal repetitive transcranial magnetic stimulation (rTMS) changes relative perfusion locally and remotely, Hum. Psychopharmacol. Clin. Exp. 14 (1999) 161–170.

[6] M.S. George, E.M. Wassermann, W.A. Williams, A. Callahan, T.A. Ketter, P. Basser, M. Hallett, R.M. Post, Daily repetitive transcranial magnetic stimulation (rTMS) improves mood in depression, Neuroreport 6 (1995) 1853–1856.

[7] A. Hausmann, G. Kemmler, M. Walpoth, S. Mechtcheriakov, K. Kramer-Reinstadler, T. Lechner, T. Walch, E.A. Deisenhammer, M. Kofler, C.I. Rupp, H. Hinterhuber, A. Conca, No benefit derived from repetitive transcranial magnetic stimulation in depression: a prospective, single centre, randomised, double blind, sham controlled "add on" trial, J. Neurol. Neurosurg. Psychiatry 75 (2004) 320–322.

[8] K. Isenberg, D. Downs, K. Pierce, D. Svarakic, K. Garcia, M. Jarvis, C. North, T.C. Kormos, Low frequency rTMS stimulation of the right frontal cortex is as effective as high frequency rTMS stimulation of the left frontal cortex for antidepressant-free, treatment-resistant depressed patients, Ann. Clin. Psychiatry 17 (2005) 153–159.

[9] N. Iwata, Y. Ugawa, Imaging functional connectivity by combining transcranial magnetic stimulation (TMS) and functional neuroimaging techniques, Clin. Electroencephalogr. 44 (2002) 80–85, in Japanese.

[10] D. Januel, G. Dumortier, C.M. Verdon, L. Stamatiadis, G. Saba, W. Cabaret, R. Benadhira, J.F. Rocamora, S. Braha, K. Kalalou, P.E. Vicaut, J. Fermanian, A double-blind sham controlled study of right prefrontal repetitive transcranial magnetic stimulation (rTMS): therapeutic and cognitive effect in medication free unipolar depression during 4 weeks, Prog. Neuropsychopharmacol. Biol. Psychiatry 30 (2006) 126–130.

[11] M. Kameyama, M. Fukuda, T. Uehara, M. Mikuni, Sex and age dependencies of cerebral blood volume changes during cognitive activation: a multichannel near-infrared spectroscopy study, Neuroimage 22 (2004) 1715–1721.

[12] E. Klein, I. Kreinin, A. Chistyakov, D. Koren, L. Mecz, S. Marmur, D. Ben-Shachar, M. Feinsod, Therapeutic efficacy of right prefrontal slow repetitive transcranial magnetic stimulation in major depression: a double-blind controlled study, Arch. Gen. Psychiatry 56 (1999) 315–320.

[13] D. Knoch, V. Treyer, M. Regard, R.M. Muri, A. Buck, B. Weber, Lateralized and frequency-dependent effects of prefrontal rTMS on regional cerebral blood flow, Neuroimage 31 (2006) 641–648.

[14] X. Li, Z. Nahas, F.A. Kozel, B. Anderson, D.E. Bohning, M.S. George, Acute left prefrontal transcranial magnetic stimulation in depressed patients is associated with immediately increased activity in prefrontal cortical as well as subcortical regions, Biol. Psychiatry 55 (2004) 882–890.

[15] C. Loo, P. Mitchell, P. Sachdev, B. McDarmont, G. Parker, S. Gandevia, Double-blind controlled investigation of transcranial magnetic stimulation for the treatment of resistant major depression, Am. J. Psychiatry 156 (1999) 946–948.

[16] C.K. Loo, P.S. Sachdev, W. Haindl, W. Wen, P.B. Mitchell, V.M. Croker, G.S. Malhi, High (15 Hz) and low (1 Hz) frequency transcranial magnetic stimulation have different acute effects on regional cerebral blood flow in depressed patients, Psychol. Med. 33 (2003) 997–1006.

[17] H. Mochizuki, Y. Ugawa, Y. Terao, K.L. Sakai, Cortical hemoglobin-concentration changes under the coil induced by single-pulse TMS in humans: a simultaneous recording with near-infrared spectroscopy, Exp. Brain Res. 169 (2006) 302–310.

[18] Z. Nahas, M. Lomarev, D.R. Roberts, A. Shastri, J.P. Lorberbaum, C. Teneback, K. McConnell, D.J. Vincent, X. Li, M.S. George, D.E. Bohning, Unilateral left prefrontal transcranial magnetic stimulation (TMS) produces intensity-dependent bilateral effects as measured by interleaved BOLD fMRI, Biol. Psychiatry 50 (2001) 712–720.

[19] Y. Noguchi, E. Watanabe, K.L. Sakai, An event-related optical topography study of cortical activation induced by single-pulse transcranial magnetic stimulation, Neuroimage 19 (2003) 156–162.

[20] T. Ohnishi, H. Matsuda, E. Imabayashi, S. Okabe, H. Takano, N. Arai, Y. Ugawa, rCBF changes elicited by rTMS over DLPFC in humans, Suppl. Clin. Neurophysiol. 57 (2004) 715–720.

[21] R.C. Oldfield, The assessment and analysis of handedness: the Edinburgh inventory, Neuropsychologia 9 (1971) 97–113.

[22] A. Oliviero, V. Di Lazzaro, O. Piazza, P. Profice, M.A. Pennisi, F. Della Corte, P. Tonali, Cerebral blood flow and metabolic changes produced by repetitive magnetic brain stimulation, J. Neurol. 246 (1999) 1164–1168.

[23] A. Pascual-Leone, B. Rubio, F. Pallardo, M.D. Catala, Rapid-rate transcranial magnetic stimulation of left dorsolateral prefrontal cortex in drug-resistant depression, Lancet 348 (1996) 233–237.

[24] A. Pascual-Leone, J. Valls-Sole, E.M. Wassermann, M. Hallett, Responses to rapid-rate transcranial magnetic stimulation of the human motor cortex, Brain 117 (1994) 847–858.

[25] J.D. Rollnik, A. Dusterhoft, J. Dauper, A. Kossev, K. Weissenborn, R. Dengler, Decrease of middle cerebral artery blood flow velocity after low-frequency repetitive transcranial magnetic stimulation of the dorsolateral prefrontal cortex, Clin. Neurophysiol. 113 (2002) 951–955.

[26] A.M. Speer, T.A. Kimbrell, E.M. Wassermann, J.D. Repella, M.W. Willis, P. Herscovitch, R.M. Post, Opposite effects of high and low frequency rTMS on regional brain activity in depressed patients, Biol. Psychiatry 48 (2000) 1133–1141.

[27] A.M. Speer, M.W. Willis, P. Herscovitch, M. Daube-Witherspoon, J.R. Shelton, B.E. Benson, R.M. Post, E.M. Wassermann, Intensity-dependent regional cerebral blood flow during 1-Hz repetitive transcranial magnetic stimulation (rTMS) in healthy volunteers studied with H215O positron emission tomography: II. Effects of prefrontal cortex rTMS, Biol. Psychiatry 54 (2003) 826–832.

[28] E.M. Wassermann, Risk and safety of repetitive transcranial magnetic stimulation: report and suggested guidelines from the International Workshop on the Safety of Repetitive Transcranial Magnetic Stimulation, June 5-7, 1996, Electroencephalogr. Clin. Neurophysiol. 108 (1998) 1–16.

[29] E. Watanabe, A. Maki, F. Kawaguchi, K. Takashiro, Y. Yamashita, H. Koizumi, Y. Mayanagi, Non-invasive assessment of language dominance with near-infrared spectroscopic mapping, Neurosci. Lett. 256 (1998) 49–52.

Neuropathology 2008; **28**, 143–150 doi:10.1111/j.1440-1789.2007.00867.x

Original Article

Changes in density of calcium-binding-protein-immunoreactive GABAergic neurons in prefrontal cortex in schizophrenia and bipolar disorder

Tsutomu Sakai,[1] Akihiko Oshima,[1] Yusuke Nozaki,[1] Itsuro Ida,[2] Chie Haga,[3] Haruhiko Akiyama,[3] Yoichi Nakazato[4] and Masahiko Mikuni[1]

Departments of [1]Psychiatry and Human Behavior and [4]Human Pathology, Gunma University Graduate School of Medicine, [2]Takasaki National Hospital, Gunma, and [3]Tokyo Institute of Psychiatry, Tokyo, Japan

There is evidence that GABAergic neurotransmission is altered in mental disorders such as schizophrenia (SCZ) and bipolar disorder (BPD). The calcium-binding proteins (CBPs) calbindin (CB), calretinin (CR), and parvalbumin (PV) are used as markers of specific subpopulations of cortical GABAergic interneurons. We examined the postmortem prefrontal cortical region (Brodmann's area 9) of patients with SCZ and BPD, and of age-matched control subjects, excluding suicide cases. The laminar density of neurons immunoreactive (IR) for three CBPs, namely CB, CR, and PV, was quantified. The densities of CB-IR neurons in layer 2 and PV-IR neurons in layer 4 in the SCZ subjects decreased compared with those in the control subjects. When CBP-IR neurons were classified according to their size, a reduction in the density of medium CB-IR neurons in layer 2 in SCZ subjects and an increase in the density of large CR-IR neurons in layer 2 in BPD subjects were observed. These results suggest that alterations in specific GABAergic neurons are present in mental disorders, and that such alterations may reflect the vulnerability toward the disorders.

Key words: bipolar disorder, calbindin, calretinin, parvalbumin, schizophrenia.

INTRODUCTION

GABAergic neurons provide both inhibitory and disinhibitory modulation of cortical and hippocampal circuits and contribute to the generation of oscillatory rhythms, discriminative information processing and the gating of sensory information within the corticolimbic system. In previous studies, it was suggested that these functions are altered in schizophrenic (SCZ) subjects.[1–3] GABAergic function also contributes to the control of impulsive and aggressive behaviors, and drugs such as carbamazepine, valproate, and lithium carbonate, which have been reported to change the levels of GABA and glutamic acid decarboxylase (GAD) activity,[4–7] have been used as mood stabilizers in the treatment of bipolar disorder (BPD) to reduce impulsive and aggressive behaviors. These drugs have also been used as adjunct therapy to antipsychotics in the treatment of SCZ.[8–10] In these reports, it was suggested that GABAergic neurotransmission is altered in mental disorders such as SCZ and BPD.

In the prefrontal cortex (PFC) of SCZ subjects, a reduced number of neurons expressing the mRNA for the 67-kDa isoform of GAD,[11,12] and a high density of $GABA_A$ receptor subunits[13,14] have been reported, whereas in the anterior cingulate cortex (ACC) of SCZ subjects, an increased number of $GABA_A$ receptors,[15] and increases in the size of GAD_{65}-immunoreactive (IR) terminals[16] are indicated. The high-intensity immunoreactivity of $GABA_A$ receptor subunits[13,14] in PFC and a reduction in the density of GAD_{65}-IR terminals in PFC and ACC[16] have been also described in BPD subjects. These findings suggest that there is a specific deficit in GABAergic inhibitory neurons in these disorders.

Correspondence: Tsutomu Sakai, MD, Department of Psychiatry and Human Behavior, Gunma University Graduate School of Medicine, 3-39-22 Showa-machi, Maebashi, Gunma 371-8511, Japan. Email: sakaitsu@med.gunma-u.ac.jp

Received 13 August 2007; revised 19 September 2007; accepted 1 October 2007.

Cortical GABAergic cells can be categorized by the colocalization of neuropeptides, including somatostatin, cholecystokinin, neuropeptide Y, and vasoactive intestinal polypeptide.[17–19] Somatostatin, neuropeptide Y, vasoactive intestinal polypeptide and cholecystokinin concentrations are reduced in SCZ subjects,[20] and neuropeptide Y mRNA expression is reduced in BPD subjects.[21,22]

GABAergic neurons can also be classified by the presence of the calcium-binding proteins (CBPs) parvalbumin (PV), calbindin (CB), and calretinin (CR).[23,24] CB, PV and CR are present in non-pyramidal GABAergic neurons, which participate in various primate cortical circuits that may differ depending on the species, cortical area and layer in which they are located. CR is found in double-bouquet neurons, bipolar cells and Cajal-Retzius cells, CB is found in neurogliaform neurons and double-bouquet cells, and PV is found in chandelier and wide arbor (basket) neurons, and each calcium-binding protein is expressed in separate populations of prefrontal cortical neurons.[25,26]

Previous studies in which these CBPs were used as markers of GABAergic neurons in the prefrontal cortex did not show consistent results: a trend towards increases in the densities of CR-IR and PV-IR neurons;[27] reductions in the densities of CB-IR neurons[28,29] and PV-IR neurons in the PFC of SCZ subjects;[28–31] and no changes in the density of CR-IR[29,31] or PV-IR[32] neurons. Similarly, a decrease in the density of CB-IR neurons[28] and no change in CBP-IR neuron density[33] were also found in the PFC of BPD subjects. However, in most of these studies, SCZ and BPD subjects including suicide subjects were examined; control subjects were not suicidal. Moreover, the number of reports on CBP-IR neurons in the postmortem brain of BPD subjects is still small.

Therefore, the following questions arise. (i) If these studies excluded suicide subjects, would there be any alterations in density and distribution of CBP-IR neurons in subjects with these disorders? (ii) Are there consistent changes in the postmortem tissue of subjects with BPD? (iii) If the CBP-IR neurons are classified according to size, are there alterations in the cellular distribution in the PFC in subjects with these disorders?

To address these points, we quantified the densities of interneurons immunoreactive for PV, CB, and CR in the prefrontal cortical region of subjects with SCZ and BPD, and of age-matched control subjects, excluding suicide subjects.

METHODS AND MATERIALS

Participants

Human brain specimens from Brodmann's area 9 (BA9) were obtained from the Tokyo Institute of Psychiatry and Matsuzawa Hospital (Tokyo, Japan). The samples were obtained from 19 subjects (5 control, 7 SCZ, and 5 BPD subjects). Diagnoses were made according to DSM-IV criteria. Detailed case summaries were provided with demographic and clinical information (see Table 1 for group summary details). Subjects with a past history of neurological diseases and those whose death was caused by suicide were excluded. This study was approved by the Ethical Committee of Tokyo Metropolitan Matsuzawa Hospital, and the specimens were provided with the consent of the patients before death or of the family.

Immunocytochemistry

Hemispheres were fixed in 10% formalin and cut in frontal sections of roughly 1 cm thickness. The slices were embedded in paraffin. From these embedded blocks, serial sections of 4 μm thickness were prepared.

Three tissue sections per subject were used in each of the three investigations. Deparaffinized sections were incubated with either polyclonal anti-CB (1 : 100 Sigma, St Louis, MO, US), polyclonal anti-CR (1 : 1000 Sigma), or polyclonal anti-PV (1 : 800 Abcam, Cambridge, UK) antibodies overnight at 4°C. Sections were processed using the

Table 1 Group summaries of demographic and clinical information on the brains donated by the Tokyo Institute of Psychiatry and Matsuzawa Hospital

Variable	Group		
	Control	BPD	SCZ
Demographics			
Age at death in years (mean ± SD)	56.8 ± 5.81	54.6 ± 9.86	47.4 ± 7.63
Gender (male : female)	2 : 3	1 : 4	3 : 4
Clinical factors			
Cause of death	3a, 2b	4a, 1d	2a, 1c, 3d, 1e
Duration of disorder in years (mean ± SD)	—	21.0 ± 18.3	29.0 ± 7.02
Past alcohol/drug abuse or dependence (no : yes)	4 : 1	5 : 0	6 : 1

The cause of death is categorized under the following headings: a, heart and respiratory failure; b, liver failure; c, renal failure; d, cancer; and e, thyroid crisis. BPD, bipolar disorder, SCZ, schizophrenia.

streptoavidin-biotin peroxidase method and a Histofine SAB-PO kit (Nichirei, Tokyo, Japan), visualized using diaminobenzidine (DAB) and intensified with osmic acid. Control sections, in which the primary antibody was omitted, were processed in parallel. Sections were counterstained with hematoxylin for 10 sec.

To identify the cytoarchitecture and cortical layers of BA9,[34] sections usually adjacent to or within 20 μm from the immunostained sections were stained with hematoxylin.

Areal density and cell size measurement

PV-, CR-, and CB-IR neurons were analyzed by two investigators (TS and AO). The methods of image and quantitative analysis were identical for each investigation.

Immunoreactive cells were plotted at 4× magnification using a Nikon microscope (Eclipse E800) equipped with an Olympus digital camera (DP 50). Using the software Viewfinder Lite ver.1.0 and Studio Lite ver.1.0 (Pixera Japan, Kanagawa, Japan), we obtained a series of contiguous images of the cortex from the pia to the gray/white matter border, from which a single composite image was formed using Adobe Photoshop CS.

Sections stained with hematoxylin for identification were analyzed using Image-J software ver.1.34 to measure cortical and laminar thicknesses and to count the number of cells in each layer. Cortical layers were distinguished on the basis of the differences in the distribution, size and shape of their neurons.[34] At each position in which data were acquired, immunoreactive cells were counted for each layer. The density of neuronal profiles was expressed as mean values (± SE) per mm^2 per layer from a total of two 1000-μm-wide cortical traverses, each from the pial surface to the white matter border. Cortical traverses were located in an area devoid of damage and blood vessels and where the pial surface was parallel to the white matter border.

We used a semiautomated threshold to identify and outline all stained cells within the composite images. The threshold of the light intensity level was selected for each image so that the glia and neurons were well outlined. Neurons were identified by the presence of a stained cytoplasm and by their generally larger shape. Glia were differentiated from neurons by their more rounded and darker appearance, and smaller shape.

For each case and section, the somal size of each cell counted was measured using Image-J software, and each IR-neuron was classified into two classes according to their size. The size range was determined using the mean and SD of the size of the cells of the control subjects as follows: medium (within mean + 1 SD), large (larger than mean + 1 SD).

Statistical analysis

The relative density of labeled neurons from the two cortical traverses was averaged for each cortical layer in each case, and the results were analyzed by two-way ANOVA followed by the Bonferroni or Tamhane test using layers and diagnoses as variables. Following this analysis, the mean densities of PV-, CB-, and CR-IR neurons in each cortical layer for each of the two patient groups were compared with those of the control group by one-way ANOVA, which enabled us to determine disease and laminar specificity.

The demographic and histological variables listed in Table 1, for example age and sex, were considered to be confounders, and were therefore included in the analysis as covariates if they differed between each group at the 10% significance level (ANOVA or χ^2 test) or if they could also be shown empirically to predict densities at the 10% significance level (Spearman's rank correlation). All statistical analyses were carried out using SPSS 12.0 software (SPSS Japan Inc., Tokyo, Japan.).

RESULTS

Identification of adjustment variables

Because no significant group differences were detected for the demographic or clinical variables at the 10% significance level (ANOVA or χ^2 test) (Table 1), these variables were not included in the analysis as covariates.

Neurons and glia

Significant reductions in neuronal density were detected by two-way ANOVA in the BPD subjects ($P = 0.038$) and SCZ ($P = 0.002$) subjects. The neuronal density determined at each layer comparison showed reductions in layer 3 (22%, $P < 0.001$), layer 4 (31%, $P < 0.001$), and layer 5/6 (28%, $P = 0.006$) in the SCZ subjects, and in layer 4 (28%, $P = 0.031$) in the BPD subjects, and even after Abercrombie correction changes in the same direction were estimated. However, no significant differences in the somal size of neurons were observed. There was no change in glial density in any of the layers in the psychiatric disorder groups compared with that in the control group, and no change in glial size was observed.

CBP-IR neurons

CB-IR neurons were present predominantly in layer 2 and the superficial layer 3. The majority of these cells corresponded to non-pyramidal neurons, and showed intense immunoreactivity, and the minority were pyramidal in shape with a low immunoreactivity (Fig. 1). CR-IR neurons also appeared to be non-pyramidal neurons that

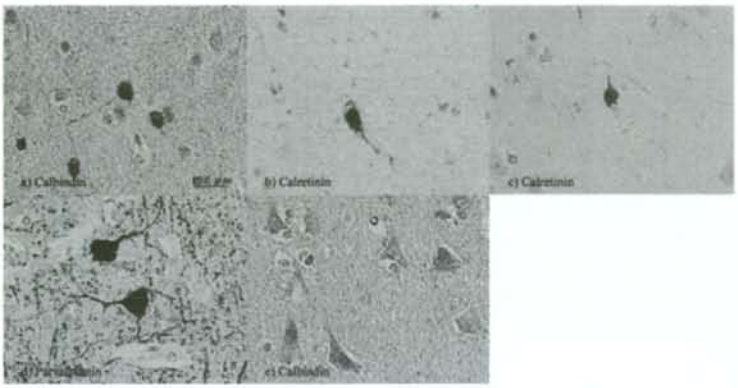

Fig. 1 Cells labeled by immunoreactivity to calbindin in layer 2 (a), calretinin in layer 1 (b) and layer 3 (c), parvalbumin in layer 3 (d), and labeled by low immunoreactivity to calbindin in layer 3 (e) of control subjects (bar = 20 μm).

Table 2 Densities (mean ± SE cells/mm²) of calcium-binding-protein-immunoreactive neurons in BA9 in schizophrenia (SCZ), bipolar disorder (BPD), and control (CON) groups

Calcium-binding protein	Cortical layer	Diagnosis					
		CON ($n = 5$)		BPD ($n = 5$)		SCZ ($n = 7$)	
		Medium	Large	Medium	Large	Medium	Large
Calbindin	1	3.40 ± 1.69	0.51 ± 0.51	0	0	0.84 ± 0.60	0
	2	64.48 ± 7.61	11.32 ± 4.01	46.20 ± 5.47	2.35 ± 1.13	32.29 ± 7.33*	0.30 ± 0.30
	3	32.14 ± 13.03	2.21 ± 0.67	13.27 ± 5.09	0.54 ± 0.41	13.80 ± 3.98	0.71 ± 0.29
	4	15.54 ± 9.81	3.27 ± 2.87	3.53 ± 2.17	0.36 ± 0.36	2.91 ± 1.24	0.28 ± 0.28
	5/6	7.34 ± 4.14	1.29 ± 1.29	2.07 ± 1.05	0.38 ± 0.25	2.82 ± 1.51	0.07 ± 0.07
Calretinin	1	18.98 ± 5.09	3.51 ± 1.37	20.15 ± 7.02	2.25 ± 0.95	4.03 ± 1.92	1.03 ± 1.03
	2	56.38 ± 6.90	5.52 ± 1.63	56.46 ± 9.07	17.11 ± 3.76*	29.47 ± 7.94	2.78 ± 1.44
	3	22.74 ± 4.81	4.26 ± 1.23	21.08 ± 2.92	7.01 ± 1.80	10.52 ± 2.86	1.29 ± 0.59
	4	7.59 ± 3.21	1.87 ± 0.88	6.18 ± 2.94	0.68 ± 0.68	4.80 ± 2.13	1.11 ± 0.96
	5/6	1.64 ± 0.74	0.12 ± 0.12	1.93 ± 0.72	0.34 ± 0.14	0.68 ± 0.19	0.17 ± 0.17
Parvalbumin	1	1.82 ± 0.91	0	2.40 ± 1.61	0	0.65 ± 0.65	0
	2	36.33 ± 6.06	1.51 ± 0.69	28.79 ± 3.19	3.03 ± 1.17	19.41 ± 5.31	0
	3	41.15 ± 3.92	9.28 ± 2.39	35.81 ± 3.89	9.48 ± 3.64	30.53 ± 3.47	3.33 ± 1.12
	4	57.60 ± 6.84	12.48 ± 3.79	60.25 ± 4.10	11.57 ± 3.33	45.10 ± 3.59	2.87 ± 1.37
	5/6	20.82 ± 2.63	2.00 ± 0.89	20.43 ± 2.99	4.36 ± 1.70	12.92 ± 1.67	0.62 ± 0.24

*$P < 0.05$.

were present in all the layers, but were predominantly present in the superficial layers such as layers 2 and 3 (Fig. 1). PV-IR neurons were mainly distributed from the intermediate to inferior layers, and consisted of some morphologically distinctive neurons, including small ovoid-type and large multipolar neurons (Fig. 1). A plexus of PV-IR material was also distributed throughout the neuropil of layers 3, 4, and 5/6 and consisted of stained processes and puncta, which have been identified as terminals principally found on dendritic spines.[35] Summaries of the mean densities and sizes for each neuronal subpopulation in each layer are shown in Table 2 and Figure 2.

CBP-IR neurons were classified into medium and large classes according to size at the data acquisition points using mean + 1 SD of the size of the cells of the control subjects as follows: CB-IR neurons, 318 μm²; CR-IR neurons, 231 μm²; PV-IR neurons, 533 μm².

Density

Neuronal density was reduced in the SCZ and BPD subjects, and this variable was included in ANOVA as a covariate for evaluating CBP-IR neuron density; however, no significant correlations were obtained between neuronal density and CBP-IR neuron density, and therefore CBP-IR neuron density was analyzed by ANOVA. Before the classification according to cell size, no significant differences were detected by two-way ANOVA between the control group and the psychiatric disorder groups, but there was a trend toward reductions in CB-IR ($P = 0.061$), CR-IR ($P = 0.061$) and PV-IR ($P = 0.093$) neuron densities in the SCZ group. The total CBP-IR neuron density in each layer was estimated, and the CB-IR neuron density in layer 2 (57%, $P = 0.007$), and PV-IR neuron density in layer 4 (32%, $P = 0.031$) in the SCZ group were reduced compared with

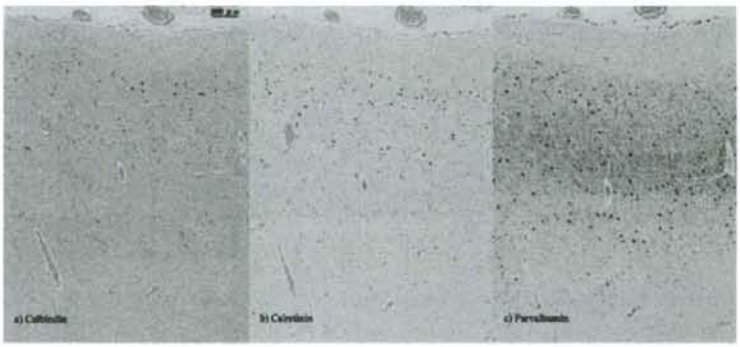

Fig. 2 Composite image showing calcium-binding protein-immunoreactive neurons. The composite images were made up of a series of contiguous images obtained individually at ×4 magnification, that were merged to form a single large image. (bar = 200 μm)

those in the control group. In the BPD group, no significant difference was noted. After classifying the cells by size, medium CB-IR neuron density was found to be reduced in layer 2 in the SCZ subjects (50%, $P = 0.018$), and large-CR-IR neuron density in layer 2 in the BPD subjects (68%, $P = 0.015$) was increased compared with those in the control subjects (Table 2). No differences in the density of any PV-IR neuron types were detected in the BPD or SCZ subjects, but trends toward decreases in large-PV-IR-neuron density in layer 4 (77%, $P = 0.075$) and in medium-PV-IR-neuron density in layer 5/6 (38%, $P = 0.089$) in the SCZ subjects were noted.

Abercrombie correction

After Abercrombie correction, the estimated CBP-IR neuron density ratios indicated the same changes as those described above. These were a reduction in medium-class CB-IR neuron density ratio in layer 2 in the SCZ subjects ($P = 0.024$), a trend toward a reduction in large-class PV-IR neuron density ratio in layer 4 in the SCZ subjects ($P = 0.075$), and an increase in large-class CR-IR neuron density ratio in layer 2 in the BPD subjects ($P = 0.017$). However, there were no significant changes in the ratios of the total counts of PV-IR neurons in layer 4, and of medium-class PV-IR neurons in layer 5/6.

DISCUSSION

IR neurons

In this study, we found significant reductions in the density of CB-IR neurons in layer 2 and PV-IR neurons in layer 4 of the PFC in SCZ subjects (in the between-layer comparison). In addition, when CBP-IR neurons were divided into two classes according to their size, a reduced density of medium-class CB-IR neurons in layer 2 in the SCZ subjects was also observed. We found no significant changes in either of the two types of PV-IR density, but there was a trend toward a reduction in large-PV-IR neuron density in layer 4 in the SCZ subjects. These results confirm those of previous studies on the PFC, which showed reductions in the density of CB-IR neurons[28,29] or PV-IR cells[28-31] and suggested no significant changes in CR-IR neuron density in the SCZ subjects.[31,36] This study supports the evidence that there is a deficit in GABAergic neurotransmission in SCZ.

No significant changes in CBP-IR neuron density between layers in the BPD subjects were found, which is consistent with the results of a report showing no changes in CBP-IR neuron density[33] in the dorsolateral PFC in BPD subjects. However, when IR cells were classified by size, there was an increased density of large CR-IR neurons in layer 2 in the BPD subjects, and also notably a non-significant but 28% reduction in CB-IR neuron density in the BPD subjects compared with the case of the control subjects (Table 2), which confirms the findings of a previous study.[28] These results suggest alterations in the cellular organization of CR-IR and CB-IR cells, and it is possible that an increase in CR-IR neuron density may be secondary to a reduction in CB-IR neuron density, or vice versa. Because we found no differences in neuronal density in layer 2 in the SCZ or BPD subjects, our findings on CBP-IR neurons may not depend on a reduction in cell number but rather on a decrease in protein expression.

Because non-suicidal subjects with psychiatric disorders were compared with control subjects, the findings in this study are free from additional effects of suicidal symptoms and actions. Suicide is the most serious outcome of mental disorders, and suicide cases usually present emotional instability and other severe symptoms immediately before death. Most previous studies compared psychiatric sample groups including suicide subjects, who amounted to half the total number of subjects or more, with control groups without any cases of suicide. When suicidal subjects were excluded, influence of mental state before suicide and of suicide actions would be avoided. The deficits in the

subpopulations of GABAergic neurons that were observed in this study may reflect cytoarchitectural abnormalities which constitute vulnerability to SCZ or BPD, but as our data are still preliminary, so a definite conclusion should be left to more rigorous and large-scale studies.

In addition, the distribution of the CBP-IR neurons classified in two types according to their size was examined, and a speculation about differences in IR-neuron activity between groups is possible. Because neuronal somal size is considered to be correlated with the extent of a cell's dendritic arborization,[37,38] a reduced neuronal somal size suggests diminished neuronal activity, and the changes in cellular organization also indicate alterations in neurotransmission. In this regard, the reductions of medium-class CB-IR neurons and large-class PV-IR neurons suggest deficits in neurotransmission between proximal neurons and between distal neurons, respectively, in SCZ in PFC (BA9), and the increase in large CR-IR neuron density may be related to the potentiation of GABAergic transmission in BPD.

Methodological and confounding factors

We determined two-dimensional, not three-dimensional, cell density. The chief problem with two-dimensional counting is that there is a possibility of overcounting and creating a bias. However, this bias can be corrected using formulae.[39] Although unbiased three-dimensional counting is superior when there are group differences in cell size, two-dimensional counting methods, which use large sampling frames, provide more accurate estimates of cell density than their three-dimensional counterparts if the confounding effect of cell size is correctly adjusted for using Abercrombie correction.[39] Another potential advantage of two-dimensional counting is that three-dimensional counting, which uses large sampling frames, makes inappropriate assumptions on complete spatial randomness for neurons, which could bias results.[40] The results of this analysis did not differ from those carried out on unadjusted data.

Because it is difficult to perform immunocytochemistry with three types of antibody at a time in thick sections which are typically used in three-dimensional counting, we used the antibody for each CBP in three separate sections. The thicknesses of these serial sections were all 4 μm, 16 μm in total, such that the size is smaller than the diameter of one neuron. Therefore, it is safely assumed that all three CBP-IR neurons are distributed in the column in which a single neuron exists.

In this study, the influence of major potential confounders on measures of CBP-IR neurons was examined. No significant differences at the 10% significance level (ANOVA or χ^2 test) were detected for the demographic or clinical variables shown in Table 1. There were also no significant differences and correlation in some other potential confounders such as postmortem interval and time from fixation to specimen making (data not shown). Therefore our data are presumably specific to each diagnostic group and not artifacts of these confounders.

Our present data suggest that there are GABAergic dysfunctions in schizophrenia and bipolar disorder. However, because GABAergic neurons are subdivided by other coexisting proteins such as somatostatin, vasointenstial polypeptide (VIP), and cholecystokinin (CCK), it is necessary to investigate these alternate subtypes of GABAergic neurons to comprehensively determine the nature of GABAergic abnormalitites in these disorders.

ACKNOWLEDGMENTS

We thank Dr Tsuchiya K of the Department of Laboratory Medicine and Pathology, Tokyo Metropolitan Hospital, Tokyo, Japan for the analysis of the brain tissues, and also Yokota M, Yamazaki H, and Isoda K of the Department of Pathology, Gunma University Graduate School of Medicine, Gunma, Japan for technical assistance. This study was partly supported by Research Grants from the Japanese Ministry of Health, Labor and Welfare.

REFERENCES

1. Saccuzzo DP, Braff DL. Information-processing abnormalities: trait- and state-dependent components. *Schizophr Bull* 1986; **12**: 447–459.
2. Braff DL, Heaton R, Kuck J *et al.* The generalized pattern of neuropsychological deficits in outpatients with chronic schizophrenia with heterogeneous Wisconsin Card Sorting Test results. *Arch Gen Psychiatry* 1991; **48**: 891–898.
3. Blackwood DH, St Clair DM, Muir WJ, Duffy JC. Auditory P300 and eye tracking dysfunction in schizophrenic pedigrees. *Arch Gene Psychiatry* 1991; **48**: 899–909.
4. Otero Losada ME, Rubio MC. Acute and chronic effects of lithium chloride on GABA-ergic function in the rat corpus striatum and frontal cerebral cortex. *Naunyn Schmiedebergs Arch Pharmacol* 1986; **332**: 169–172.
5. Ahluwalia P, Grewaal DS, Singhal RL. Brain gabaergic and dopaminergic systems following lithium treatment and withdrawal. *Prog Neuropsychopharmacol* 1981; **5**: 527–530.
6. Gottesfeld Z. Effect of lithium and other alkali metals on brain chemistry and behavior. I. Glutamic acid and GABA in brain regions. *Psychopharmacologia* 1976; **45**: 239–242.

7. Weiss S, Kemp DE, Bauce L, Tse FW. Kainate receptors coupled to the evoked release of 3H-gamma-aminobutyric acid from striatal neurons in primary culture: potentiation by lithium ions. *Mol Pharmacol* 1990; **38**: 229–236.
8. Citrome L, Levine J, Allingham B. Changes in use of valproate and other mood stabilizers for patients with schizophrenia from 1994 to 1998. *Psychiatr Serv* 2000; **51**: 634–638.
9. Citrome L, Jaffe A, Levine J, Allingham B. Use of mood stabilizers among patients with schizophrenia, 1994–2001. *Psychiatr Serv* 2002; **53**: 1212.
10. Berle JO, Spigset O. Are mood stabilizers beneficial in the treatment of schizophrenia? *Tidsskr Nor Laegeforen* 2005; **125**: 1809–1812.
11. Akbarian S, Kim JJ, Potkin SG *et al.* Gene expression for glutamic acid decarboxylase is reduced without loss of neurons in prefrontal cortex of schizophrenics. *Arch Gen Psychiatry* 1995; **52**: 258–266.
12. Volk DW, Austin MC, Pierri JN, Sampson AR, Lewis DA. Decreased glutamic acid decarboxylase67 messenger RNA expression in a subset of prefrontal cortical gamma-aminobutyric acid neurons in subjects with schizophrenia. *Arch Gen Psychiatry* 2000; **57**: 237–245.
13. Ishikawa M, Mizukami K, Iwakiri M, Hidaka S, Asada T. Immunohistochemical and immunoblot study of GABA (A) alpha1 and beta2/3 subunits in the prefrontal cortex of subjects with schizophrenia and bipolar disorder. *Neurosci Res* 2004; **50**: 77–84.
14. Impagnatiello F, Guidotti AR, Pesold C *et al.* A decrease of reelin expression as a putative vulnerability factor in schizophrenia. *Proc Natl Acad Sci USA* 1998; **95**: 15718–15723.
15. Benes FM, Vincent SL, Alsterberg G, Bird ED, SanGiovanni JP. Increased GABAA receptor binding in superficial layers of cingulate cortex in schizophrenics. *J Neurosci* 1992; **12**: 924–929.
16. Benes FM, Todtenkopf MS, Logiotatos P, Williams M. Glutamate decarboxylase (65) -immunoreactive terminals in cingulate and prefrontal cortices of schizophrenic and bipolar brain. *J Chem Neuroanat* 2000; **20**: 259–269.
17. Somogyi P, Hodgson AJ, Smith AD, Nunzi MG, Gorio A, Wu JY. Different populations of GABAergic neurons in the visual cortex and hippocampus of cat contain somatostatin- or cholecystokinin-immunoreactive material. *J Neurosci* 1984; **4**: 2590–2603.
18. Demeulemeester H, Vandesande F, Orban GA. Immunocytochemical localization of somatostatin and cholecystokinin in the cat visual cortex. *Brain Res* 1985; **332**: 361–364.
19. Demeulemeester H, Vandesande F, Orban GA, Brandon C, Vanderhaeghen JJ. Heterogeneity of GABAergic cells in cat visual cortex. *J Neurosci* 1988; **8**: 988–1000.
20. Gabriel SM, Davidson M, Haroutunian V *et al.* Neuropeptide deficits in schizophrenia vs. Alzheimer's disease cerebral cortex. *Biol Psychiatry* 1996; **39**: 82–91.
21. Caberlotto L, Hurd YL. Reduced neuropeptide Y mRNA expression in the prefrontal cortex of subjects with bipolar disorder. *Neuroreport* 1999; **10**: 1747–1750.
22. Kuromitsu J, Yokoi A, Kawai T *et al.* Reduced neuropeptide Y mRNA levels in the frontal cortex of people with schizophrenia and bipolar disorder. *Brain Res Gene Expr Patterns* 2001; **1**: 17–21.
23. Celio MR. Calbindin D-28k and parvalbumin in the rat nervous system. *Neuroscience* 1990; **35**: 375–475.
24. Demeulemeester H, Arckens L, Vandesande F, Orban GA, Heizmann CW, Pochet R. Calcium binding proteins and neuropeptides as molecular markers of GABAergic interneurons in the cat visual cortex. *Exp Brain Res* 1991; **84**: 538–544.
25. DeFelipe J. Types of neurons, synaptic connections and chemical characteristics of cells immunoreactive for calbindin-D28K, parvalbumin and calretinin in the neocortex. *J Chem Neuroanat* 1997; **14**: 1–19.
26. Conde F, Lund JS, Jacobowitz DM, Baimbridge KG, Lewis DA. Local circuit neurons immunoreactive for calretinin, calbindin D-28k or parvalbumin in monkey prefrontal cortex: distribution and morphology. *J Comp Neurol* 1994; **341**: 95–116.
27. Tooney PA, Chahl LA. Neurons expressing calcium-binding proteins in the prefrontal cortex in schizophrenia. Prog Neuropsychopharmacol. *Biol Psychiatry* 2004; **28**: 273–278.
28. Beasley CL, Zhang ZJ, Patten I, Reynolds GP. Selective deficits in prefrontal cortical GABAergic neurons in schizophrenia defined by the presence of calcium-binding proteins. *Biol Psychiatry* 2002; **52**: 708–715.
29. Reynolds GP, Zhang ZJ, Beasley CL. Neurochemical correlates of cortical GABAergic deficits in schizophrenia: selective losses of calcium binding protein immunoreactivity. *Brain Res Bull* 2001; **55**: 579–584.
30. Beasley CL, Reynolds GP. Parvalbumin-immunoreactive neurons are reduced in the prefrontal cortex of schizophrenics. *Schizophr Res* 1997; **24**: 349–355.
31. Reynolds GP, Beasley CL. GABAergic neuronal subtypes in the human frontal cortex – development and deficits in schizophrenia. *J Chem Neuroanat* 2001; **22**: 95–100.
32. Woo TU, Miller JL, Lewis DA. Schizophrenia and the parvalbumin-containing class of cortical local circuit neurons. *Am J Psychiatry* 1997; **154**: 1013–1015.

33. Reynolds GP, Beasley CL, Zhang ZJ. Understanding the neurotransmitter pathology of schizophrenia: selective deficits of subtypes of cortical GABAergic neurons. *J Neural Transm* 2002; **109**: 881–889.
34. Rajkowska G, Goldman-Rakic PS. Cytoarchitectonic definition of prefrontal areas in the normal human cortex. I. Remapping of areas 9 and 46 using quantitative criteria. *Cereb Cortex* 1995; **5**: 307–322.
35. DeFelipe J, Jones EG. Parvalbumin immunoreactivity reveals layer IV of monkey cerebral cortex as a mosaic of microzones of thalamic afferent terminations. *Brain Res* 1991; **562**: 39–47.
36. Daviss SR, Lewis DA. Local circuit neurons of the prefrontal cortex in schizophrenia: selective increase in the density of calbindin-immunoreactive neurons. *Psychiatry Res* 1995; **59**: 81–96.
37. Hayes TL. Lewis DA. Hemispheric differences in layer III pyramidal neurons of the anterior language area. *Arch Neurol* 1993; **50**: 501–505.
38. Lund JS, Lund RD, Hendrickson AE, Bunt AH, Fuchs AF. The origin of efferent pathways from the primary visual cortex, area 17, of the macaque monkey as shown by retrograde transport of horseradish peroxidase. *J Comp Neurol* 1975; **164**: 287–303.
39. Abercrombie M, Johnson ML. Quantitative histology of Wallerian degeneration. I. Nuclear population in rabbit sciatic nerve. *J Anat* 1946; **80**: 37–50.
40. Benes FM, Lange N. Two-dimensional versus three-dimensional cell counting: a practical perspective. *Trends Neurosci* 2001; **24**: 11–17.

Available online at www.sciencedirect.com
ScienceDirect
Journal of Psychiatric Research 42 (2008) 443–450
JOURNAL OF PSYCHIATRIC RESEARCH
www.elsevier.com/locate/jpsychires

Relationship between age at onset and magnetic resonance image-defined hyperintensities in mood disorders

K. Takahashi [a], A. Oshima [a,*], I. Ida [b], H. Kumano [a], N. Yuuki [c], M. Fukuda [a], M. Amanuma [d], K. Endo [d], M. Mikuni [a]

[a] *Department of Psychiatry and Human Behavior, Gunma University Graduate School of Medicine, 3-39-22 Showa-machi, Maebashi, Gunma 371-8511, Japan*
[b] *Takasaki National Hospital, Gunma, Japan*
[c] *Gunma Prefectural Psychiatric Medical Center, Gunma, Japan*
[d] *Department of Diagnostic Radiology and Nuclear Medicine, Gunma University Graduate School of Medicine, Gunma, Japan*

Received 22 December 2006; received in revised form 3 May 2007; accepted 3 May 2007

Abstract

Objectives: To examine in patients with mood disorders the relationship of age at onset with the location and degree of MRI-defined brain hyperintensities.
Method: Fifty-two patients diagnosed as having mood disorders and 14 controls participated in the study. Brain MR images were analyzed according to semiquantitative ratings for the anatomical distribution and severity of T2-weighted hyperintensities. We compared these hyperintensities among the three age- and sex-matched groups of late-onset mood disorder patients (LOM), early-onset mood disorder patients (EOM), and controls. The time since the onset of disorder was significantly longer in the EOM than in the LOM group. We also conducted linear multiple regression analysis using the severity of hyperintensities as dependent variable to determine whether the clinical features correlate with vascular pathology.
Results: As for deep white matter hyperintensity (DWMH), LOM exhibited higher ratings than EOM; as for brain areas, significant between-group differences were detected in the bilateral frontal areas and in the left parieto-occipital area. No significant difference was observed between EOM and controls. As for periventricular hyperintensity, there was no difference among the three groups. We obtained a significant regression model to predict DWMH ratings; age, number of ECTs, and LOM were selected as significant variables.
Conclusion: The present study suggests that the time since the onset of disorder does not affect the development of white matter lesions, but that white matter lesions are associated with late-onset mood disorders. The frontal areas and the left parieto-occipital area would be important for the development of late-onset mood disorders.

Keywords: Cerebrovascular lesion; Bipolar disorder; Major depressive disorder; Illness vulnerability; Risk factors; Hypertension

1. Introduction

Regarding major depression, there are differences in various clinical indices depending on the age at onset, such as clinical symptoms (Baldwin and Tomenson, 1995; Salloway et al., 1996; Krishnan et al., 1995), degree of cognitive impairment (Salloway et al., 1996; Alexopoulos et al., 1993), clinical course (Hickie et al., 1997; Alexopoulos et al., 1996), and suicide risk (Lyness et al., 1992). Hopkinson (1964) reported that the risk of depression in the first-degree relatives of depressed patients was 20% in the early-onset depression group compared with 8.3% in the late-onset depression group over 50 years of age. Because similar conclusions have been made by Schultz (1951) and Post (1975), it may be assumed that genetic factors exert greater effects in early-onset depression than in late-onset depression.

* Corresponding author. Tel.: +81 27 220 8190; fax: +81 27 220 8187.
E-mail address: aoshima@med.gunma-u.ac.jp (A. Oshima).

0022-3956/$ - see front matter © 2007 Elsevier Ltd. All rights reserved.
doi:10.1016/j.jpsychires.2007.05.003

Bipolar affective disorders (BPADs) have also been studied in terms of subgroups divided according to the age at onset (Leboyer et al., 2005). Strober (1992) reviewed eight studies and found that relatives of early-onset BPAD patients are 1.1–3.9 times more likely to develop affective disorder than are the relatives of late-onset BPAD probands, indicating that the onset of early-onset BPADs is strongly associated with genetic factors.

Physical factors, particularly organic brain factors, are highly involved in mood disorders occurring at older ages (Rodin and Voshart, 1986). In the late 1980s, it was reported that patients with late-onset depression had significantly more complications of cerebrovascular disorders including asymptomatic cerebral infarction than those without any depression (Krishnan et al., 1988; Baldwin, 1993; Soares and Mann, 1997). It was previously reported that there were many patients who developed depression after having a stroke (poststroke depression) (Folstein et al., 1977). These observations led to the view that the pathophysiology of late-onset depression may be closely associated with cerebrovascular conditions; hence, the concept of vascular depression was proposed by Alexopoulos et al. (1997) and Krishnan et al. (1997). In large-scale epidemiologic studies that followed, de Groot et al. (2000) found in their Rotterdam Scan Study that subjects with severe white matter lesions showed a 3–5-fold risk of depression. There has been reported of an increase in the severity of deep white matter lesions in BPADs as well. They are more frequently observed in late-onset than in early-onset BPADs (Altshuler et al., 1995).

Factors such as age (de Leeuw et al., 2001; Manolio et al., 1994), elevated blood pressure (de Leeuw et al., 2002), diabetes (Longstreth et al., 2001), and cardiac arrhythmia (Ylikowski et al., 1995) have been reported as risk factors of white matter lesions. In the general population, however, there is less evidence that vascular risk factors are a major cause of depression (Thomas et al., 2004). There have been reports that there is no link between depression symptoms and elevated blood pressure (Jones-Webb et al., 1996; Friedman and Bennet, 1977) nor between a history of hypertension or of coronary heart disease and a history of depression (Steffens et al., 2002). In the Rotterdam Study, however, Tiemeier et al., who examined vasomotor reactivity in the middle cerebral artery using CO_2 inhalation, reported that the depression group exhibited a lower vasomotor reactivity than healthy controls (Tiemeier et al., 2002) and that arterial stiffness significantly correlated with the severity of depression (Tiemeier et al., 2003). Thomas et al. (2001) found in their postmortem study that atheromas in major vessels (coronary arteries, carotid arteries, and aortas) were significantly more severe in the depression group than in the normal group.

In summary, differences in pathogenesis and pathophysiology presumably exist between the early-onset and the late-onset mood disorder groups. Also, depression itself can be a risk factor for vascular lesions (Baldwin, 2005), which led to the hypothesis that depression exacerbates cerebrovascular lesions with aging (Lenze et al., 1999). However, there have been few studies in which subjects within age-matched groups were compared, that is, between patients with late-onset mood disorders, those with early-onset ones, and normal elderly subjects with regard to brain areas.

In this study, we hypothesized that patients with late-onset mood disorders would show more severe cerebrovascular lesions, especially in the frontal area, than those with early-onset mood disorders in the same present age range and with longer illness period than those with late-onset mood disorders, because there have been a number of studies indicating frontal lobe dysfunction in depressed patients. Therefore, we compared MRI-defined subcortical high intensities with regard to brain areas by dividing the mood disorders patients of the same age range into the late-onset and early-onset mood disorder groups and by including normal elderly subjects as the control. We also conducted linear multiple regression analysis using the severity of subcortical lesions as dependent variable to determine whether the clinical features of mood disorders and medical comorbidities correlate with vascular pathology.

2. Subjects and method

2.1. Subjects

This is a retrospective study conducted in the Department of Neuropsychiatry, Gunma University Hospital in Japan. One hundred and three outpatients or inpatients with mood disorders underwent MRI scan from 2003 to 2006. Patients who met the DSM-IV criteria for any types of dementia ($n = 15$) or showed symptoms of cerebral infarction ($n = 8$) or were aged fewer than 50 ($n = 28$) were excluded. After this exclusion, subjects consisted of 52 patients who met the DSM-IV criteria for major depressive disorder (24 females, 18 males; 9 mild, 18 moderate, 12 severe with psychotic feature, 3 severe without psychotic feature) or bipolar I disorder (1 females, 5 males) or bipolar II disorder (1 females, 3 males). In addition, we added to the study group 14 psychiatrically normal elderly controls older than 50 years old (EC; 8 females, 6 males) according to a comprehensive history and psychiatric interview. By setting the age at onset of 50 years as the cut-off for late onset vs. early onset, we classified 29 patients into the late-onset mood disorder (LOM) group and 23 patients into the early-onset mood disorder (EOM) group.

The characteristics of the subjects are shown in Table 1. There were no significant differences in age (one-way ANOVA: $F = 1.81$, $df = 2$, $P = 0.172$) or gender (two-tailed chi-square test: $\chi^2 = 2.18$, $df = 2$, $P = 0.337$) among the LOM, EOM and EC groups. Ages at onset were significantly lower in the EOM group than those in the LOM group (two-tailed nonpaired t-test: $t = 9.39$, $df = 36.26$, $P < 0.001$). There was also no significant difference in the percentage of patients with BPADs between the LOM

Table 1
Characteristics of subjects

	Patient			Controls
	Combined	Late onset	Early onset	
N	52	29	23	14
Female, *n* (%)	26 (50.0)	17 (58.6)	9 (39.1)	8 (57.1)
Age, mean year (SD)	60.8 (7.0)	62.2 (5.3)	58.9 (8.5)	63.1 (9.4)
Age at onset, mean year (SD)	49.5 (13.2)	59.0 (6.2)[a]	37.6 (9.4)	–
Bipolar, *n* (%)	10 (19.2)	5 (17.2)	5 (21.7)	–

[a] Late onset vs. early onset: $T = 9.39$, df = 36.26, $P < 0.001$.

and EOM groups (two-tailed Fisher's exact test: $P = 0.734$).

The Institutional Review Board of Gunma University Hospital approved this study, and written informed consent was obtained from all the subjects and/or their families.

2.2. MRI procedure and image analysis

We obtained the following images of the subjects using a 1.5-T MAGNETOM Symphony Maestro class, (Siemens Medical Solutions, Erlangen, Germany): axial T_2-weighted images (TR 3800ms; TE 90ms) and axial T_1-weighted images (TR 500ms; TE 14ms). The slices of images were 5-mm thick, with a 2.0-mm interslice gap, and the images of the entire brain parenchyma were obtained. An experienced psychiatrist (K.T. or A.O.) independently evaluated the MR images without knowledge of subjects' status. Each T2-weighted MR image was evaluated in terms of periventricular hyperintensity (PVH) and deep white matter hyperintensity (DWMH) on the basis of Fazekas criteria (Fazekas et al., 1987), obtaining semiquantitative ratings for brain hyperintensities. Typical images of Fazekas criteria are shown in Fig. 1. PVH was rated as follows: 0 = absent, 1 = "caps" or pencil-thin lining, 2 = smooth "halo", and 3 = irregular PVH extending into the deep white matter. DWMH was rated as follows: 0 = absent, 1 = punctate foci, 2 = beginning confluence of foci, and 3 = large confluent area. To understand the functional anatomical role of the lesions, the regions of interest were classified into the following four areas in each hemisphere. Eight areas were thus evaluated similarly to the four-stage Fazekas DWMH criteria. The areas of interest were the following: (1) the frontal area (right and left, FR and FL, respectively), the frontal lobe anterior to the central sulcus; (2) the parieto-occipital area (right and left, POR and POL, respectively), consisted of the parietal and occipital lobe together; (3) the temporal area (right and left, TR and TL, respectively), the temporal lobe (the border between the parieto-occipital and temporal lobes was approximated as the line drawn from the posterior part of the Sylvian fissure to the trigone areas of the lateral ventricles); and (4) the basal ganglia (right and left, BGR and BGL, respectively), including the striatum, globus pallidus, thalamus, internal and external capsules, and insula. Periventricular lesions were not added to the respective regional scores in order to focus on short association fibers within hemispheres and to exclude commissural fibers and projection fibers that are more densly found in the periventricular area. The interrater reliability exceeded 0.95. There was no discrepancy of more than 1 point between the two evaluators with the given criteria.

2.3. Statistical analysis

All analyses were performed using SPSS (SPSS Inc., Chicago, Illinois; version 12.0J). We compared between the LOM and EOM groups using Fisher's exact test in terms of the presence or absence of psychotic features, history of suicide attempt, history of delirium, a family history

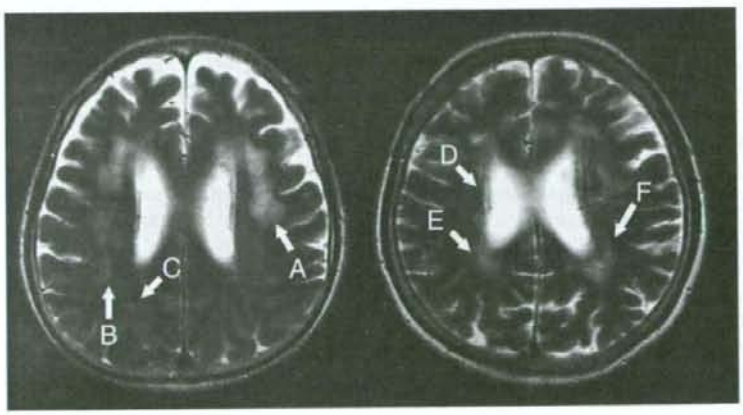

Fig. 1. Typical images of Fazekas ratings. *Note.* DWMH grade: A = grade 3, B = grade 2, C = grade 1; PVH grade: D = grade 1, E = grade 2, F = grade 3.

of psychiatric disorders within the second-degree, history of electroconvulsive therapy (ECT), habitual smoking, habitual alcohol drinking, obesity (Body Mass Index: BMI > 25), the percentage of patients who have had a history of complications of diabetes mellitus (DM), hypertension (HT), hyperlipemia (HL), ischemic heart disease (IHD) and cardiac arrhythmia (CA). We also compared time since the onset of a disorder, the number of episodes (depressive and manic episodes), the total number of episodes, the number of suicide attempts, the number of ECTs and doses of antidepressants (Imipramine equivalent dose) between the groups using the nonpaired *t*-test. *P*-values were truncated at 0.05 using the two-tailed test in Fisher's exact test and the nonpaired *t*-test. As for the Fazekas ratings of PVH and DWMH in FR, FL, POR, POL, TR, TL, BGR, and BGL in the LOM, EOM, and EC groups, we compared them by one-way ANOVA followed by Tuckey's test.

For these 52 patients, we also conducted linear multiple regression analysis using the DWMH scores as dependent variable. Using stepwise method, independent valuables were selected from dimensional scores; age, age at onset, time since the onset of a disorder, the number of episodes (depressive, manic and total episodes), the number of suicide attempts, the number of ECTs and doses of antidepressants, and from categorical scores; LOM, sex, bipolar, psychotic features, delirium, family history of psychiatric disorders, habitual smoking, habitual alcohol drinking, obesity, DM, HT, HL, IHD, CA. Significant variables were entered if the *P*-value of each variable was under 0.05, and deleted for $P > 0.10$.

3. Results

3.1. Early-onset mood disorders vs. late-onset mood disorders vs. elderly controls

3.1.1. Clinical background and medical comorbidities

The results of comparison of clinical features between the LOM and EOM groups are shown in Table 2. The time since the onset of disorder was significantly longer in the EOM group ($T = -7.36$, df = 26.62, $P < 0.001$). The percentage of patients with obesity was higher in the EOM group ($P = 0.015$). There was not any significant difference in the other items.

3.1.2. Fazekas semiquantitative ratings

As for the scores of DWMH and PVH (Fig. 2, Table 3), there was a significant difference in DWMH ($F = 4.67$, df = 2, $P = 0.013$) between the groups, but not in PVH ($F = 2.43$, df = 2, $P = 0.096$). Pathological changes in LOM were significantly more severe than those in EOM ($P = 0.016$). Compared with EC, LOM showed more severe pathological changes, but not significantly ($P = 0.096$). There was no difference between EOM and EC ($P = 0.946$).

In terms of regional DWMH (Table 3), there was a significant ANOVA results in FR ($F = 4.52$, df = 2,

Table 2
Clinical background, medical comorbidities and *P*-values for comparison between late-onset mood disorder ($n = 29$) and early-onset mood disorder ($n = 23$) groups

		LOM	EOM	*P*-value
N		29	23	
Time since onset of disorder, mean year (SD)		3.3 (4.1)	21.3 (11.2)	<0.001[a]
Depressive episodes, mean number (SD)		1.6 (0.8)	6.0 (12.4)	0.096[a]
Manic episodes, mean number (SD)		0.3 (0.9)	1.0 (2.2)	0.195[a]
Total episodes, mean number (SD)		1.9 (1.4)	7.1 (12.8)	0.063[a]
With psychotic features, *n* (%)		12 (41.4)	4 (17.4)	0.077[b]
Suicide attempts, mean number (SD)		0.2 (0.7)	0.22 (0.4)	0.948[a]
With suicide attempt history, *n* (%)		3 (10.3)	5 (21.7)	0.441[b]
With delirium history, *n* (%)		5 (17.2)	8 (34.8)	0.201[b]
Family history of psychiatric disorders, *n* (%)		9 (31.0)	13 (56.5)	0.092[b]
ECTs, mean number (SD)		12.8 (48.8)	7.9 (21.0)	0.656[a]
With ECT history, *n* (%)		8 (27.6)	7 (30.4)	1.000[b]
Antidepressant agent, Imipramine equivalent dose mg/day (SD)		116.0 (86.5)	107.2 (91.7)	0.724[a]
Habitual smoking, *n* (%)		8 (27.6)	6 (26.1)	1.000[b]
Habitual alcohol drinking, *n* (%)		6 (20.7)	5 (21.7)	1.000[b]
Obesity, *n* (%)[c]		1 (4.2)	7 (35.0)	0.015[b]
Medical comorbidities	DM, *n* (%)	5 (17.2)	2 (8.7)	0.444[b]
	HT, *n* (%)	10 (34.5)	5 (21.7)	0.369[b]
	HL, *n* (%)	1 (3.4)	2 (8.7)	0.577[b]
	IHD, *n* (%)	1 (3.4)	0 (0.0)	1.000[b]
	CA, *n* (%)	3 (10.3)	1 (4.3)	0.621[b]

Note. LOM, late-onset mood disorder group; EOM, early-onset mood disorder group; ECT, electroconvulsive therapy; DM, diabetes mellitus; HT, hypertension; HL, hyperlipemia; IHD, ischemic heart disease; CA, cardiac arrhythmia.

[a] *P*-values for two-tailed nonpaired *t*-test.

[b] *P*-values for two-tailed Fisher's exact test.

[c] Comparison between 24 patients of LOM and 20 patients of EOM.

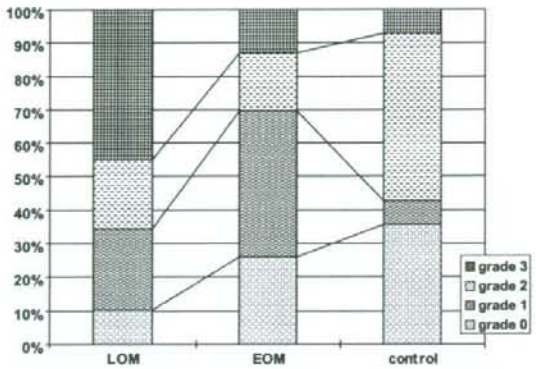

Fig. 2. The distribution of Fazekas DWMH ratings in LOM, EOM, and control groups. *Note.* LOM, late-onset mood disorder group; EOM, early-onset mood disorder group.

$P = 0.015$), FL ($F = 3.29$, df = 2, $P = 0.044$), and POL ($F = 6.35$, df = 2, $P = 0.003$). In the post hoc tests between LOM and EOM, significant differences were detected in FR ($P = 0.033$), FL ($P = 0.043$), and POL ($P = 0.003$). Between LOM and EC, a significant difference was detected in FR ($P = 0.048$).

3.2. Linear multiple regression analysis using the DWMH ratings as dependent variable

Results of linear multiple regression analysis are shown in Table 4. We obtained a significant regression model to predict the DWMH ratings ($F = 16.5$, $P < 0.001$); age, number of ECTs, and LOM were selected as significant variables ($t = 5.5$, -3.7, and 2.5; $P < 0.001$, 0.01, and 0.05, respectively).

4. Discussion

This study is unique in that we compared white matter lesions with regard to brain areas among the age- and gender-matched LOM, EOM and EC groups that include major depressive disorder and bipolar disorder. As for DWMH, LOM exhibited a higher rating than EOM; as for brain areas, significant between-group differences were detected in bilateral frontal areas and in the left parieto-occipital area. LOM, but not EOM, tended to show more severe pathological changes than the EC group, and there was a significant difference in the severity of changes in the right frontal areas. As for PVH, there was no difference among the three groups. In the linear multiple regression

Table 3
Fazekas ratings and *P*-values for comparison among late-onset mood disorder ($n = 29$), early-onset mood disorder ($n = 23$), and elderly control ($n = 14$) groups

	LOM	EOM	Controls	One-way ANOVA		Post hoc test *P*-value (Tukey HSD)		
				F-value	*P*-value	LOM vs. EOM	LOM vs. controls	EOM vs. controls
DWMH, mean (SD)	2.00 (1.07)	1.17 (0.98)	1.29 (1.07)	4.67	0.013	0.016*	0.096	0.946
PVH, mean (SD)	1.28 (1.22)	0.61 (1.08)	0.71 (1.14)	2.43	0.096	0.105	0.301	0.961
FR, mean (SD)	1.76 (1.18)	1.00 (1.00)	0.93 (0.83)	4.52	0.015	0.033*	0.048*	0.978
FL, mean (SD)	1.72 (1.19)	0.96 (1.07)	1.14 (1.03)	3.29	0.044	0.043*	0.253	0.875
POR, mean (SD)	1.14 (1.06)	0.48 (0.85)	0.86 (0.86)	3.09	0.052	0.041	0.637	0.472
POL, mean (SD)	1.31 (1.07)	0.43 (0.79)	0.64 (0.74)	6.35	0.003	0.003*	0.073	0.782
TR, mean (SD)	0.83 (1.00)	0.48 (0.90)	0.50 (0.52)	1.21	0.305	0.340	0.495	0.997
TL, mean (SD)	0.86 (1.03)	0.57 (0.95)	0.64 (0.63)	0.75	0.498	0.490	0.749	0.967
BGR, mean (SD)	0.62 (0.86)	0.43 (0.79)	0.29 (0.47)	0.97	0.385	0.664	0.380	0.836
BGL, mean (SD)	0.66 (0.97)	0.43 (0.84)	0.21 (0.43)	1.36	0.264	0.618	0.249	0.721

Note. LOM, late-onset mood disorder group; EOM, early-onset mood disorder group; DWMH, deep white matter hyperintensity; PVH, periventricular hyperintensity; FR, right frontal area; FL, left frontal area; POR, right parieto-occipital area; POL, left parieto-occipital area; TR, right temporal area; TL, left temporal area; BGR, right basal ganglia; BGL, left basal ganglia.
* One-way ANOVA $P < 0.05$ and post hoc test $P < 0.05$.

Table 4
Prediction of the DWMH ratings

	Dependent valiable	Variables entered	Standardized coefficients	*t*	R^2	*F*
$n = 52$	DWMH ratings				0.52	16.5***
df (1,44)		Age	0.61	5.5***		
		number of ECTs	−0.40	−3.7**		
		LOM group	0.27	2.5*		

Note. Multiple linear regression, stepwise method, DWMH: deep white matter hyperintensities, ECT: electro convulsive therapy, LOM: late-onset mood disorder.
* $P < 0.05$.
** $P < 0.01$.
*** $P < 0.001$.